EXPERIMENTAL EVALUATION OF PI TUNING TECHNIQUES FOR FIELD ORIENTED CONTROL OF PERMANENT MAGNET SYNCHRONOUS MOTORS

B. Zigmund[3], A. Terlizzi[1], X. T. Garcia[2], R. Pavlanin[3], L. Salvatore[1]

[1]*Politecnico di Bari, Dipartimento di Elettrotecnica ed Elettronica, V. Orabona 4, 70125 Bari, Italy, salvatore@poliba.it*
[2]*University of Glamorgan, School of Electronics, CF37 1DL Pontypridd, Wales, UK, xdeltoro@glam.ac.uk*
[3]*University of Zilina, Faculty of Electrical Engineering, Department of Mechatronics and Electronics, Univerzitna 1, 010 26 Zilina, SK, brano.zigmund@gmail.com, pavlanin@fel.utc.sk*

Summary This paper presents the experimental evaluation of a commonly used methodology to tune the PI regulators of the Field Oriented Control (FOC) strategy for Permanent Magnet Synchronous Motors (PMSMs). The methodology used is based on the Absolute Value Optimum (AVO) and Symmetric Optimum (SO) criterions. These methods employ a simplified model of the plant to be controlled. Due to the complexity and non-linearities present in the FOC PMSM drive some divergence between the ideal response and the real results will occur. In this paper a comparison between simulated and experimental results is carried out to evaluate the goodness of the solution obtained. The divergences observed between simulations and the results obtained in the experimental setup are shown and it is attempted to justify the causes of them. Overall it is concluded that the method provides a satisfactory initial commissioning of the PI regulators for the drive system under study.

1. INTRODUCTION

PID regulators are widely employed in industry due to their satisfactory behaviour in most of the control applications. One of the most important engineering tasks during the commissioning of control system is the parametric optimization of the regulators to obtain the desired control response [1].

Different methods can be employed to perform the tuning of the PID regulators. A possible classification of these methods can be as follows:

- Experimental methods based on the identification of certain response characteristics of the system. The Ziegler-Nichols open and closed loop methods are an example of these methods [2].
- Mathematical model based methods. These methods employ a mathematical model that approximates the behaviour of the system [1, 3, 4].
- Optimization techniques. By means of a merit function that can be evaluated in a test, a number of solutions consisting on different sets of parameters is evaluated. At the end the best-performing solution is found. Different techniques can be used to perform the search of the best solution [5, 6].

In the field of electrical drives PI regulators are also employed for motor control. The structure and an equivalent transfer function of this controller are shown in Fig. 1. The variables to be controlled are generally position, speed, torque, current or voltage. The fact that the measurement of these signals can contain considerable noise makes the PI structure without the derivative part more suitable. One example of application where PI regulators are employed is the FOC strategy for PMSM drives.

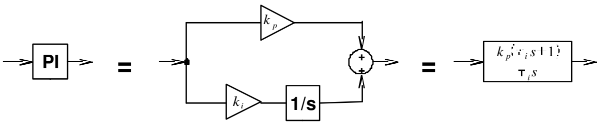

Fig. 1. PI controller structure and transfer function

This paper presents the application of two popular methods for tuning the PI regulators of the FOC PMSM drive: the AVO and SO criterions [3, 7]. The model of the PMSM is presented together with the FOC control scheme. The AVO and SO criterions are explained and applied for the system under study. Finally some simulated and experimental tests are performed in order to evaluate the solution obtained.

2. PMSM FOC

The model of the PMSM in a rotating *d-q* frame fixed to the rotor is given by the following equations:

$$\psi_{sd} = L_{sd} i_{sd} + \Psi \tag{1}$$

$$\psi_{sq} = L_{sq} i_{sq} \tag{2}$$

$$v_{sd} = R_s i_{sd} + L_{sd} \frac{di_{sd}}{dt} - \omega_r L_{sq} i_{sq} \tag{3}$$

$$v_{sq} = R_s i_{sq} + L_{sq} \frac{di_{sq}}{dt} + \omega_r \left(L_{sd} i_{sd} + \Psi \right) \tag{4}$$

$$\Gamma_e = \frac{3}{2} P \left(\psi_{sd} i_{sq} - \psi_{sq} i_{sd} \right) \tag{5}$$

where ψ_{sd}, ψ_{sq}, v_{sd}, v_{sq}, i_{sd} and i_{sq} are respectively the motor fluxes, voltages and currents in *d-q* axes; ω_r is the electrical angular speed, Γ_e is the electromagnetic torque, Ψ is the flux of the permanent magnet and P is the number of pole pairs. R_s is the stator resistance and the stator inductance can be divided into two different components L_{sd} and L_{sq} due to the particularities of the PMSM. The model is completed by the mechanical equation, which is defined as:

$$J \frac{d\omega_m}{dt} = \Gamma_e - \Gamma_l - B\omega_m \tag{6}$$

$$\omega_r = P\omega_m \tag{7}$$

where J is the inertia of the motor and coupled load, Γ_l is the load torque, B is the friction coefficient and ω_m is the mechanical angular speed.

Similarly to induction motors, in PMSMs a decoupled control of the torque and flux magnitudes can be achieved, emulating a DC motor, by means of the FOC strategy. This is done using the *d-q* transformation that separates the components *d* and *q* of the stator current responsible for flux and torque production respectively [8]. Due to the presence of the constant flux of the permanent magnet, there is no need to generate flux by means of the i_{sd} current, and this current can be kept equal to zero value, which in turns decreases the stator current and increases the efficiency of the drive. The control scheme of the FOC strategy is shown in Fig. 2.

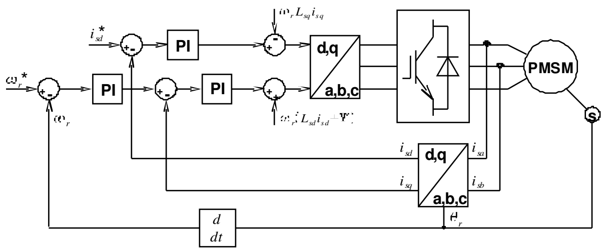

Fig. 2. FOC control scheme of PMSM

The control system is divided into three different loops: the *d* loop, which controls the flux, the *q* loop, which controls the torque and the speed control loop. The *d* loop performs the control of i_{sd} with a current PI regulator. The reference value is 0. The *q*-axis control system contains two control loops in cascade. The inner loop controls the torque by means of controlling i_{sq} with a current PI regulator. The fact that the torque can be controlled by means of i_{sq} comes from the following simplification of (5), valid for Surface Mounted (SM) PMSM:

$$\Gamma_e = \frac{3}{2} P\Psi i_{sq} \tag{8}$$

The reference for this inner loop is given by the outer loop, which contains a speed PI regulator.

From the voltage equations of the PMSM model (3) and (4) it can be seen that *d* and *q* axes are not completely independent and there are coupling terms which depend on the current from the other axis. To achieve completely independent regulation it is necessary to cancel the effect of these coupling terms at the output of the current PI regulator. With the use of decoupling it is achieved the linearization of the control system as well as higher dynamics. This decoupling action can be seen in Fig. 2 [9, 10].

3. PI TUNING WITH THE AVO AND SO CRITERIONS

In order to obtain a satisfactory control performance it is necessary to adjust the parameters of the PI regulators included in the FOC scheme. In the field of electrical drives two methods are frequently employed in this parametric optimization: the AVO and SO criterions [3, 7]. The AVO criterion can be applied to design both current regulators, while the SO can be employed to design the speed regulator shown in Fig. 2 [3]. These two methods employ an approximate transfer function of the system to be controlled. Some modelling and parameter identification of the system are therefore needed.

The AVO method assumes the system's transfer function in open loop of the following form [1]:

$$G(s) = \frac{1}{2\tau_\Sigma s(1+\tau_\Sigma s)} \tag{9}$$

On the other hand, the SO method considers the system's open loop transfer function as follows:

$$G(s) = \frac{1+4\tau_\Sigma s}{8\tau_\Sigma^2 s^2 (1+\tau_\Sigma s)} \tag{10}$$

where τ_Σ is sum of all small delays in loop. Both methods can be applied when the τ_Σ is much smaller than the time constant of the system. The step response of both transfer functions in closed loop incorporating the PI regulator designed using the AVO and SO criterions is as shown in Fig. 3. Table 1 presents the main features of the step responses obtained with both methods.

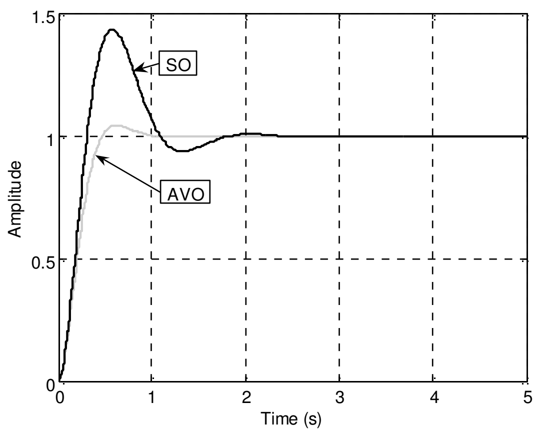

Fig. 3. AVO and SO characteristic step responses

Tab. 1. Step responses for AVO and SO methods

	AVO	SO
Rise Time	4.7 τ_Σ	3.1 τ_Σ
Settling time (2%)	8.4 τ_Σ	16.5 τ_Σ
Overshoot	4.3%	43.4%
Phase Margin	65.5°	37°

If both methods are compared it can be said that the SO is faster regarding disturbance rejection, which makes it suitable for the speed loop. On the other hand AVO has a smaller settling time and lower overshoot, which makes it appropriate to have quicker and more accurate inner loops [3].

a) Current loop PI (i_{sd} and i_{sq} control)

In order to design the regulator an approximated transfer function has to be defined according to the AVO criterion. First of all, the existing delays in the system need to be taken into account. These delays in the case of a motor drive are due to the digital implementation of the control (which implies the sampling of signals), the use of filters, the processing of the control algorithm and the use of Pulse Width Modulators (PWM). Fig. 4 shows the block diagram of the current control in closed loop with all the delays considered.

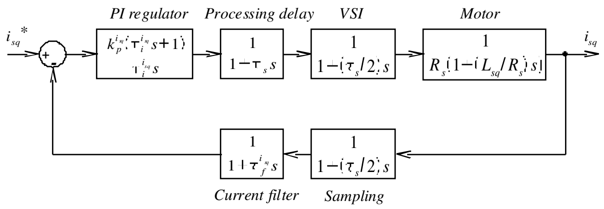

Fig. 4. Current loop block diagram

To make it possible to apply the AVO criterion, the feedback delays must be transferred to the forward path. The resulting block diagram is shown in Fig. 5.

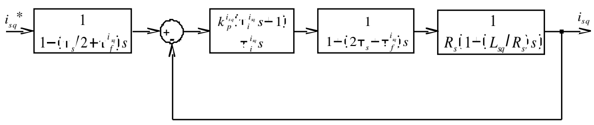

Fig. 5. Simplified block diagram of the current loop

The following approximation can be made due to fact that $\tau_s = \tau_f^{i_{sq}}$:

$$G(s) = \frac{1}{(1+\tau_s s)(1+(\tau_s/2)s)(1+(\tau_s/2)s)(1+\tau_f^{i_{sq}} s)} \quad (11)$$

$$G(s) \approx G^{'}(s) = \frac{1}{1+(2\tau_s + \tau_f^{i_{sq}})s} \quad (12)$$

In order to adapt the transfer function to the definition of the AVO method, the PI regulator time constant has to be equal to time constant of the plant. This in turns will decrease order of open loop transfer function.

$$\tau_i^{i_{sq}} = \frac{L_{sq}}{R_s} \quad (13)$$

$$G_{open}^{i_{sq}}(s) = \frac{1}{\frac{L_{sq}}{k_p^{i_{sq}}} s(1+(2\tau_s+\tau_f^{i_{sq}})s)} = \frac{1}{2\tau_\Sigma^{i_{sq}} s(1+\tau_\Sigma^{i_{sq}} s)} \quad (14)$$

Finally the values for $k_p^{i_{sq}}$ and $k_i^{i_{sq}}$ can be calculated as follows:

$$\tau_\Sigma^{i_{sq}} = 2\tau_s + \tau_f^{i_{sq}}; \quad k_p^{i_{sq}} = \frac{L_{sq}}{2\tau_\Sigma^{i_{sq}}}; \quad k_i^{i_{sq}} = \frac{k_p^{i_{sq}}}{\tau_i^{i_{sq}}} \quad (15)$$

The resulting closed loop transfer function is of the second order type. Because second order transfer functions can be approximated by a first order transfer function with the same settling time, the inner loop can be approximated as follows:

$$G_{close}^{i_{sq}}(s) = \frac{1}{1+2\tau_\Sigma^{i_{sq}} s} \quad (16)$$

In order to tune the PI current regulator in d axis it can be followed the same procedure described, but in this case using the inductance in d axis L_{sd} .

b) Speed loop PI

The speed loop is designed by means of the SO method. As in the current loop, the speed loop contains some delays that need to be defined. For this loop, it is common to use a sampling time ten times higher than the sampling time of the current loop. Fig. 6 shows the transfer function of the speed loop with all the delays considered and incorporating the inner q axis current loop transfer function defined in (16).

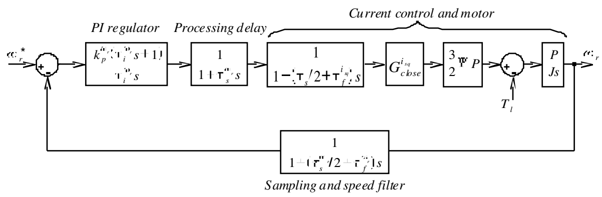

Fig. 6. Speed loop block diagram

A similar design process as in the AVO method is followed to adapt the transfer function to the SO criterion in the speed control loop. For simplicity the load torque and friction terms are neglected. The simplified block diagram passing the feedback delays to the forward loop and grouping all the delay is shown in Fig. 7.

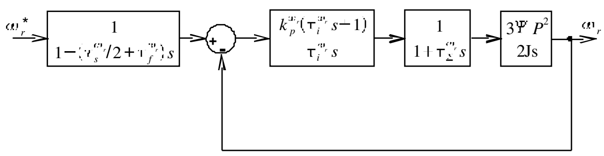

Fig. 7. Simplified speed loop block diagram

The sum of all delays in the forward loop τ_Σ^{ω} is defined as:

$$\tau_\Sigma^{\omega_r} = \frac{3}{2}\tau_s^{\omega_r} + \tau_f^{\omega_r} + 2\tau_\Sigma^{i_{sq}} - \tau_f^{i_{sq}} - \frac{\tau_s}{2} \quad (17)$$

and the resulting open loop transfer function has the appropriate form to apply the SO method:

$$G_{open}^{\omega_r}(s) = \frac{1+\tau_i^{\omega_r} s}{2J\dfrac{\tau_i^{\omega_r}}{3\Psi P^2 k_p^{\omega_r}} s^2 (1+\tau_\Sigma^{\omega_r} s)} = \frac{1+4\tau_\Sigma^{\omega_r} s}{8(\tau_\Sigma^{\omega_r})^2 s^2 (1+\tau_\Sigma^{\omega_r} s)} \quad (18)$$

Finally the values of the regulator can be obtained as follows:

$$\tau_i^{\omega_r} = 4\tau_\Sigma^{\omega_r}; \quad k_p^{\omega_r} = \frac{J}{3\Psi P^2 \tau_\Sigma^{\omega_r}}; \quad k_i^{\omega_r} = \frac{k_p^{\omega_r}}{\tau_i^{\omega_r}} \quad (19)$$

4. SIMULATED AND EXPERIMENTAL RESULTS

The methods described in the previous section have been employed to tune the i_{sd} and i_{sq} current regulators (AVO criterion) and the speed regulator (SO criterion). The resulting PI regulators have been tested using a simulation model and also an experimental setup. The experimental setup consists on a *Siemens 1KF7* PMSM with the characteristics shown in Table 2, a *Danfoss VLT5006* power converter and a *DSPACE DS1103* control board.

Tab. 2. PMSM characteristics (Siemens 1KF7)

Nominal Output Power (P_n)	2135W
Nominal Speed (ω_n)	3000rpm
Nominal Torque (M_n)	6.8N·m
Nominal Current (I_n)	4.4A
Number of pole pairs (P)	4
Stator resistance (R_s)	1.09Ω
Stator inductance (L_{sd} and L_{sq})	0.0124H
Inertia (J)	4.15e^{-4} Kg·m^2
Permanent Magnet Flux (Ψ)	0.1821Wb

The resulting set of control parameters calculated are shown in Table 3.

Tab. 3. Calculated PI parameters

PI regulator	k_p	k_i	Output Saturation
i_{sd}	8.86	778.6	$2\sqrt{2}I_n$
i_{sq}	8.86	778.6	$2\sqrt{2}I_n$
ω_r	0.0934	3.18	$V_{DC}/\sqrt{3}$

Some additional information regarding the control is shown in Table 4.

Tab. 4. Additional control parameters

Sampling time of current (τ_s)	100µs
Sampling time of speed ($\tau_s^{\omega_r}$)	1ms
DC-link Voltage (V_{DC})	$380\sqrt{2}$
Current filter time constant	500µs
Speed filter time constant	5ms

The first test performed consists on the speed step response. A comparison between the ideal response obtained employing the AVO method and the simulated and experimental results is shown in Fig. 8. It can be seen that simulated and experimental results are very similar. In both cases the overshoot is smaller than the ideal response. This is due to the friction term of the mechanical equation (6) that increases the damping of the system. It can be also appreciated the noise present in the experimental response and a higher settling time.

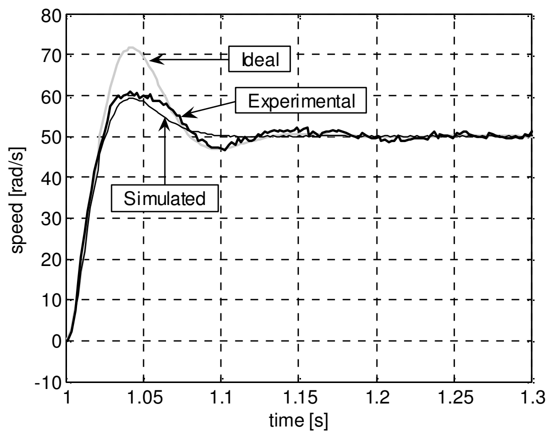

Fig. 8. Comparative step responses

The next test implemented is a speed profile which performs a speed reversal. Fig. 9 and Fig. 10 show the simulated and experimental results. The variables shown are the motor electrical speed (ω_r), the currents (i_{sd} and i_{sq}), and two phase currents (i_{sa} and i_{sb}).

The simulated and experimental results are also very similar for the speed profile test. These results illustrate a satisfactory tracking of the speed profile. The load torque in this test is only due to the friction. It can be seen how the i_{sd} is kept to zero except for the transients where some current peaks are produced.

Figures 10 and 11 show the simulated and experimental results respectively to the tracking of an i_{sq} profile. For this test the speed PI is eliminated and the reference for i_{sq} is given by a profile which includes a torque reversal. It can be seen that the experimental results present more oscillation and distortion caused by the noise of the real system and the operation of the power converter.

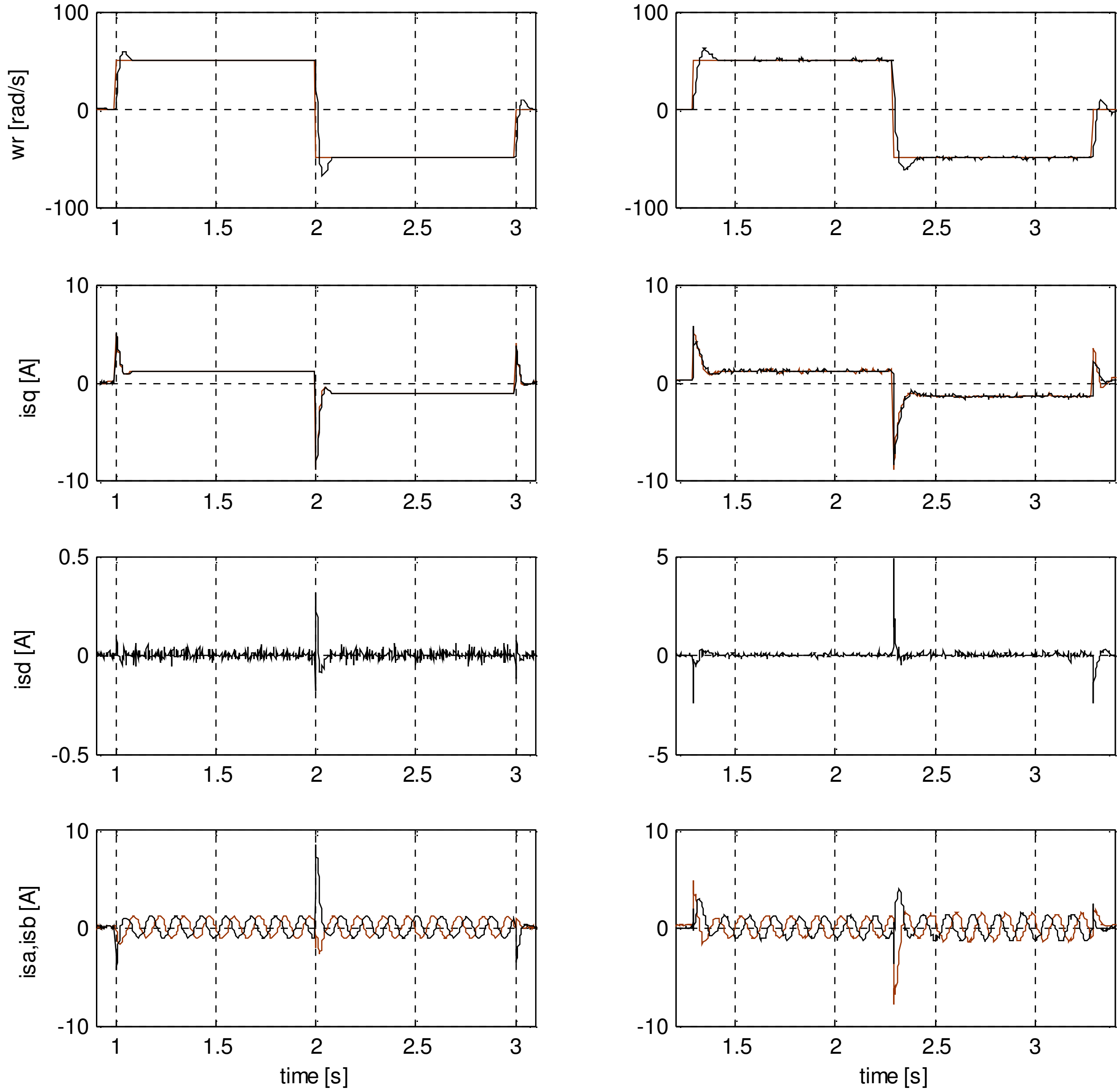

Fig. 9. Simulated (left) and experimental (right) result for the speed profile test

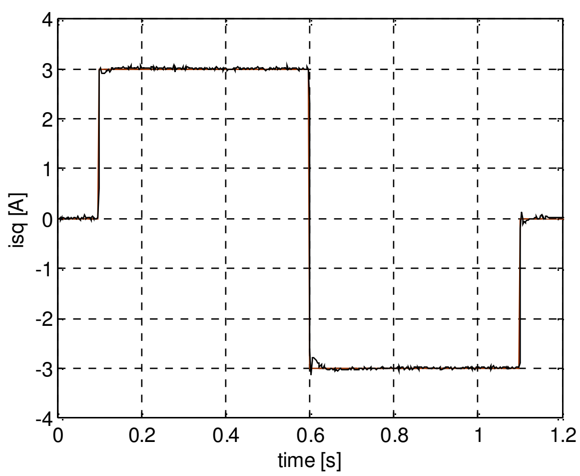

Fig. 10. Simulated results for the i_{sq} profile test

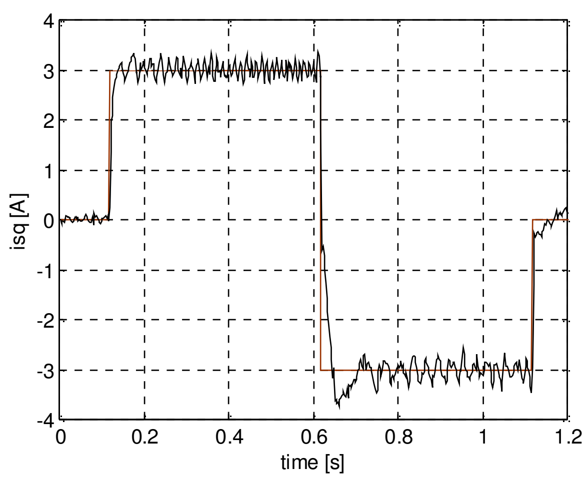

Fig. 11. Experimental results for the i_{sq} profile test

The final test presented has been carried out only in simulation to illustrate the effect of the load torque on the speed response. It can be seen that increasing the load torque results on a bigger rise time due to the saturation of the speed PI regulator outputs. The level of the saturation therefore influences the response time of the speed loop. Fig. 12 shows the speed response with 3 different levels of load torque.

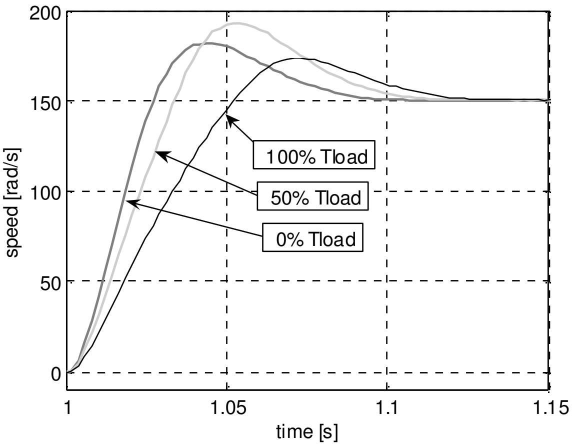

Fig. 12. Comparative step responses for different load torque conditions

5. CONCLUSION

This paper presents the experimental and simulated performance of the PI tuning AVO and SO methods applied to a FOC PMSM drive. The procedure to obtain the parameters of the PI regulators has been described for this application. The results of the different dynamic tests presented show a satisfactory control response for the speed and current loops. Overall the tuning methods employed seem to provide a valid solution for the initial commissioning of the drive system under study.

In addition the simulation model employed has proved to be very accurate and the similarity with the experimental results is very high. Any divergences observed between simulated and experimental results are due to: noise in the real setup, inaccuracy of the motor and load parameters and the operation of the converter.

Acknowledgements

This research project has been supported by a Marie Curie Early Stage Research Training Fellowship of the European Community's Sixth Framework Programme under contract number MEST-CT-2004-504243 Electrical Energy Conversion and Condition.

REFERENCES

[1] K.J. Aström and T. Hägglund: *PID Controllers: Theory, Design, and Tuning,* 2nd ed. Research Triangle Park, NC: Instrum. Soc. Amer., 1995.

[2] J.G. Ziegler and N.B. Nichols: *Optimum settings for automatic controllers*, Trans. ASME, vol. 64, pp. 759–768, Nov. 1942.

[3] J. H. H. Gross, J. Hamann and G. Wiegartner, *Electrical Feed Drives in Automation: Basics, Computation, Dimensioning*, Munich, Germany: Siemens Aktiengesellschaft, 2001.

[4] A. O'Dwater: *Handbook of PI and PID controller tuning rules*, Imperial College Press, London, 2003.

[5] K.J. Aström and T. Hägglund: *Advanced PID Control*, ISA, 2006.

[6] C.-C. Yu: *Autotuning of PID controllers*, New York: Springer-Verlag, 1999.

[7] L. Szklarski, K. Jarack and A. Horodecki: *Electric Drive Systems Dynamics. Selected Problems*, Studies in Electrical and Electronic Engineering 37. Elsevier, 1990

[8] R. Krishnan: *Electronic Motor Drives: Modeling, Analysis and Control*, Upper Saddle River, New Jersey, USA: Prentice Hall, Feb. 2001.

[9] D. W. Novotny, T. A. Lipo: *Vector Control and Dynamics of AC Drives*, Oxford University Press, 1996.

[10] P. Balazovic: *6F8300 Hybrid Controller used in Control of Electromechanical Brake*, Freescale Semiconductors, Application Notes, 1999.